Comparative Study of Zr/Te Co-Doped $MgTiO_3$: Structural, Electronic, and Optical Properties with Potential Applications

Hajar Motahhir[1,2], *Abdellah* Bouzaid[1,2], *Younes* Ziat [1,2], *Hamza* Belkhanchi[1,2], *Ayoub* Fatihi[1,2], *Youssef* Jouad[1,2], *Charaf* Laghlimi[2,3] *and Zakaryaa* Zarhri[4]

[1]Engineering and Applied Physics Laboratory (EAPL), Superior School of Technology, Sultan Moulay Slimane University, Beni Mellal, Morocco
[2]The Moroccan Association of Sciences and Techniques for Sustainable Development, Beni Mellal 23000, Morocco
[3]ERCI2A, FSTH, Abdelmalek Essaadi University, Tetouan, Morocco
[4]SECIHTI-Faculty of Chemical Sciences and Engineering, The Autonomous University of the State of Morelos (UAEM), Morelos, Cuernavaca, 62209, Mexico

Abstract. This study investigates the structural, electronic, and optical properties of pristine and Zr/Te co-doped $MgTiO_3$ using first-principles calculations based on density functional theory (DFT). The calculations were performed within the full-potential linearized augmented plane wave (FP-LAPW) method implemented in the WIEN2k code. Structural optimization was carried out using the generalized gradient approximation (GGA), while the Tran–Blaha modified Becke–Johnson (TB-mBJ) potential was employed to obtain improved electronic and optical properties. The optimized lattice parameter of pristine $MgTiO_3$ was found to be a = 3.8427 Å. The calculated band gap of undoped $MgTiO_3$ is 2.93 eV, confirming its wide-band-gap semiconducting nature with predominant ultraviolet absorption. Upon Zr and Te co-doping, the band gap significantly decreases to 1.15 eV for $Mg_8Ti_7Zr_1O_{23}Te_1$ and further to 0.64 eV for $Mg_8Ti_7Zr_1O_{22}Te_2$ due to dopant-induced electronic states near the Fermi level. Electronic structure analysis reveals strong hybridization between Te-p, O-p, Ti-d, and Zr-d orbitals, leading to band gap narrowing and a transition toward a direct band gap character. Optical calculations based on the complex dielectric function show a pronounced red shift of the absorption edge from the ultraviolet to the visible region, accompanied by an increase in the static dielectric constant and optical conductivity at low photon energies. These results demonstrate that Zr/Te co-doping effectively tunes the electronic structure and enhances visible-light absorption in $MgTiO_3$, highlighting its potential for optoelectronic and energy-related applications.

1. Introduction:

The development of advanced functional materials is a key driver for emerging technologies in electronics, optoelectronics, and energy conversion. Among these

materials, oxide perovskites have attracted considerable attention due to their structural flexibility, thermal stability, and tunable electronic properties [1, 2, 3], rendering them viable choices for applications like capacitors, resonators, and PV devices.

On the other hand, the oxide perovskites have relatively low absorption in the visible region. Recently, elemental doping/codoping has emerged as an alternative to enhance the performance of these compounds. $MgTiO_3$ is of interest due to the high stability of the structure as well as the favorable electronic properties of the compound. Codoping of $MgTiO_3$ with Zr on the Ti site and Te on the oxygen site can simultaneously optimize the cationic as well as the anionic lattices of the compound. Substitution of Ti^{4+} ions by Zr4+ ions can create lattice distortions as well as affect the conduction band of the compound, while the presence of Te can add more states to the p-band of the compound. These effects can reduce the bandgap of the compound, thus enhancing the visible region absorption as well as the separation of the charge carriers, which is necessary for photovoltaic as well as PC applications [4, 5].

$MgTiO_3$, an ilmenite-structured perovskite with high dielectric constant, low dielectric loss, and superior thermal stability, shows an intrinsic band gap of 3.4–3.7 eV, restricting the absorption of light within the range of the electromagnetic spectrum. The electronic and optical properties of $MgTiO_3$ have to be engineered through doping to precisely calculate the structural parameters in the state of equilibrium.

Magnesium titanate ($MgTiO_3$), an ilmenite-type perovskite demonstrates a high dielectric constant, minimal dielectric loss, and superior thermal stability. Its intrinsic band gap (approximately 3.4–3.7 eV) limits visible-light absorption, motivating efforts to tailor its electronic and optical properties through doping.

Other studies on codoping with Se and Zr [6] reported that this converts $MgTiO_3$ from an indirect band gap of 2.93 eV to a direct band gap of 2.159 to 1.726 eV. This improves optical conductivity and visible-light absorption and gives a good match between the band edges and the redox potential of water, leading to greater H_2 and O_2 evolution. $MgTiO_3$ with Se/Zr doping may therefore be a good choice for uses to create hydrogen with solar energy or for optoelectronic tools. When appropriately modified, $MgTiO_3$ is a promising candidate for PV and light- emitting devices, as well as plasma displays, flat-panel displays, solid-state lighting, and optical applications [7]. Furthermore, its elevated dielectric constant and minimal dielectric loss render $MgTiO_3$ appropriate for dielectric resonators in integrated circuits and wireless communication systems, and global positioning systems [8, 9]. In addition, the low dielectric loss and high thermal stability render $MgTiO_3$ an attractive material for ceramic capacitors and resonators operating at high frequencies.

Recent advances in the design of doped titanate perovskites have demonstrated that co-doping is an effective strategy to tailor their optoelectronic and photocatalytic properties. In particular, the work of Bouzaid et al. [10] on Zr/Te co-doped $ATiO_3$ (A = Ca, Sr) revealed a significant band gap reduction and improved visible-light absorption, making these materials promising for solar-driven hydrogen production and optoelectronic applications. Similarly, Bouzaid et al. [6] reported that Se/Zr co-doping in $ATiO_3$ perovskites induces impurity states near the band edges, enhancing optical absorption and charge carrier separation. These studies highlight the key role of transition metal and

chalcogen co-doping in modulating the electronic structure through orbital hybridization effects. In this context, the present work extends these investigations to $MgTiO_3$ by exploring Zr/Te co-doping, aiming to further understand and optimize the relationship between dopant-induced electronic states and optoelectronic performance.

In the first part of this paper, the optoelectronic properties of undoped $MgTiO_3$ and Zr/Te co-doped $Mg_8Ti_7Zr_1O_{23}Te_1$ and $Mg_8Ti_7Zr_1O_{22}Te_2$ compounds are investigated using DFT based on the GGA-mBJ potential. The optimized crystal structure yields a lattice constant of a = 3.8427 Å. The calculated band gaps for $MgTiO_3$, $Mg_8Ti_7Zr_1O_{23}Te_1$, and $Mg_8Ti_7Zr_1O_{22}Te_2$ are 2.93 eV, 1.15 eV, and 0.64 eV, respectively, indicating the effectiveness of Zr and Te codoping in tuning the electronic properties of $MgTiO_3$.

The present work seeks to provide insights into the structural and optoelectronic properties of $MgTiO_3$. The role of codoping Zr and Te dopants in improving the optoelectronic properties of $MgTiO_3$ is discussed in detail, and a plausible way to design materials for advanced electronics and photonics is provided.

2. Computational method:

DFT inside the FP-LAPW approach, as implemented in the WIEN2k code, was used to examine the structural and optoelectronic characteristics of both undoped $MgTiO_3$ and Zr/Te co-doped $MgTiO_3$. For the cubic perovskite structure, the primitive unit cell belongs to the space group Pm-3m (No. 221). A 2 × 2 × 2 supercell containing 40 atoms ($Mg_8Ti_8O_{24}$) was constructed to model doping concentrations. Co-doping was carried out using Zr and S replacements in two configurations: (i) 12.5% Zr and 4.16% Te and (ii) 12.5% Zr and 8.33% Te, with Zr replacing Ti and Te replacing O. In addition, utilizing the GGA, the atomic locations and unit-cell geometry were optimized. The optoelectronic properties were calculated using the TB-mBJ exchange–correlation potential. To overcome the well-known band-gap underestimation of standard GGA. The wave functions were expanded in the interstitial region using a plane-wave cutoff defined by $RMT \times K_{max} = 7$. The RMT was optimized to avoid any overlap between muffin-tin spheres. For Mg, Ti, Zr, O, and Te elements, the chosen muffin-tin radii were 2.42, 1.80, 1.92, 1.71, and 1.85 a.u., respectively.

The Brillouin zone was sampled using the Monkhorst–Pack scheme along the high-symmetry path. For the primitive unit cell, a 10 × 10 × 10 k-point mesh was employed. For the 2 × 2 × 2 supercell, a mesh containing 1000 k points was used for geometry optimization, while the same dense k-point sampling was adopted to calculate high-resolution electronic and optical properties. SCF cycles were considered converged when the total energy and total charge density reached thresholds of 10^{-5} Ry and 10^{-4} e, respectively. Furthermore, VESTA was utilized to visualize the crystal structure of the materials [11].

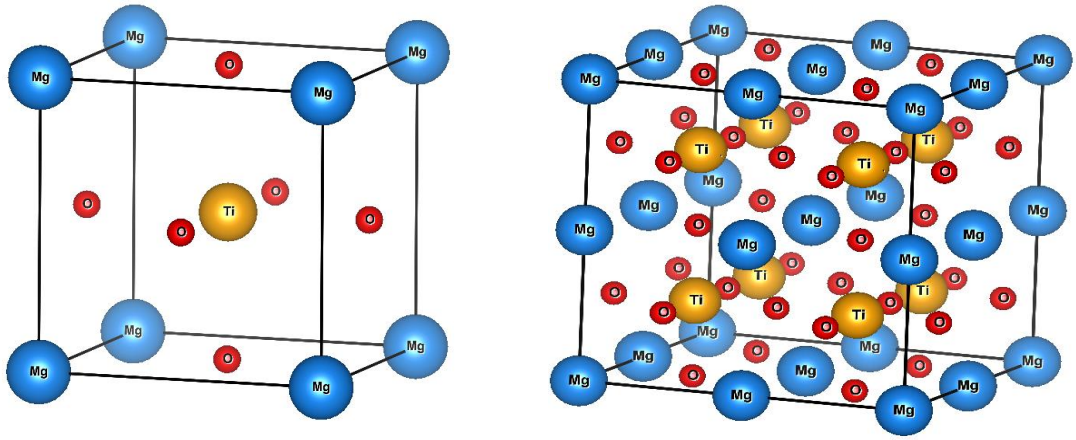

a) **b)**

Figure 1: Crystal structure of $MgTiO_3$ includes (a) the unit cell and (b) the 2 × 2 × 2 supercell used for co-doping.

3. Results and discussion:

3.1 Structural properties:

Magnesium titanate ($MgTiO_3$) belongs to the perovskite-type family, characterized by a cubic crystal structure within the Pm-3m space group (no. 221). In the ideal unit cell, the Mg atoms occupy the corners at coordinates (0, 0, 0), the Ti atoms are positioned at the center (1/2, 1/2, 1/2), and the O atoms are located at the face-centered positions (1/2, 1/2, 0). To investigate co-doping effects, a 2*2*2 supercell was constructed where one Ti^{4+} cation is replaced by Zr^{4+} and two O^{2-} anions are substituted by Te^{2-} atoms, as illustrated in Figure 1. Despite local lattice distortions caused by the larger ionic radii of the dopants, the structural integrity of the perovskite framework remains intact, enabling the optimization of the material for optoelectronic applications.To properly identify the equilibrium structural characteristics, total energy was calculated as a function of unit cell volume. The total energy–volume data were fitted using the Birch–Murnaghan equation of state [12], expressed as Equation (1).

$$E(V) = E_0 + \frac{B_0 V}{B_0'}\left[\frac{\left({}^{V_0}/_{V}\right)^{B_0'}}{B_0'-1} + 1\right] - \frac{B_0 V_0}{B_0'-1} \quad (1)$$

Here, E(V) is the total energy of the system corresponding to a specific volume V, whereas E_0 is the minimum energy corresponding to the equilibrium volume V_0. In addition, B_0 is the bulk modulus of the system and has a pressure derivative denoted by B'. The above equation helps us understand the stability of the system, and hence, the robustness of the system is assessed. Figure 2 shows the correlation between the total energy of $MgTiO_3$ and its volume. The minimum of the curve identifies the equilibrium lattice constant a = 3.8427 Å, which is in good agreement with available theoretical studies. Additionally, the calculated formation energy (Ef = -3.05 eV/atom) confirms the thermodynamic stability of $MgTiO_3$, consistent with previous literature [13].

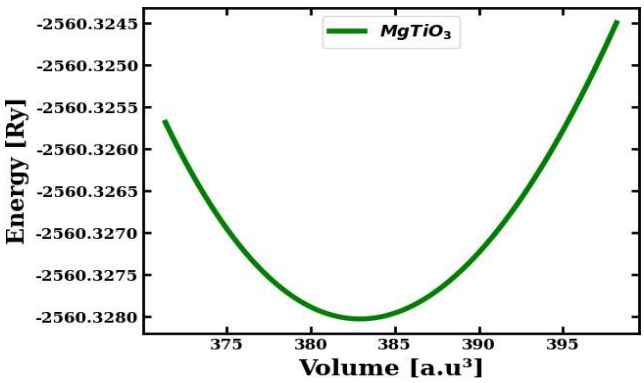

Figure 2: Fluctuation of the total energy of $MgTiO_3$ in relation to unit cell volume.

3.2 Electronic properties

Band structures of pristine and (Zr, Te) co-doped $MgTiO_3$ in their electronic configuration were calculated using TB-mBJ exchange-correlation functions. The energy dispersion was also examined along high-symmetry directions in the first Brillouin zone of the material's unit cell, while setting EF = 0 eV as shown in Figure 3.

Table 1 summarizes the calculated Eg of all materials. The codoped material exhibited a reduced Eg compared to the undoped $MgTiO_3$ (Table 1). This is because the inclusion of the electronic states of the dopant in the compound's energy structure occurs due to the fact that the compounds used for doping in the present study were present in the interstitial position and thus alter the density of the states present in the compound's structure. The optoelectronic properties of the compound. For the pristine compound $MgTiO_3$, the compound has an indirect energy gap structure, and the VBM for the compound occur at the L-point, while the for the compound occur at the Γ-point in the Brillouin zone. Calculated band gap energy for the compound using the TB-mBJ functional has the value 2.93 eV and agrees well with the earlier findings for the compound having the titanate perovskite structure [6]. This relatively wide band gap indicates that undoped $MgTiO_3$ predominantly absorbs ultraviolet radiation.

Upon simultaneous substitution of Ti by Zr and O by Te, a pronounced reduction in the band gap energy is obtained. As summarized in Table 1, the band gap decreases to 1.15 eV for $Mg_8Ti_7Zr_1O_{23}Te_1$ and further narrows to 0.64 eV for $Mg_8Ti_7Zr_1O_{22}Te_2$. This band gap narrowing originates from the appearance of dopant induced electronic states within the forbidden gap. In particular, the Te-5p orbitals introduce states near the top of the VB, while the Zr-4d states strongly hybridize with the Ti-3d orbitals at the bottom of the CB.

Moreover, the co-doped systems exhibit a transition from an indirect to a direct band gap, with the VBM and CBM located at the Γ point. This transition can be attributed to dopant-induced modifications in the local crystal field environment and enhanced orbital hybridization, which alter the electronic symmetry of the host lattice. The emergence of a direct band gap is highly desirable for optoelectronic applications, as it facilitates efficient optical transitions and improves charge carrier generation.

Thus, the present modification and narrowing of the band gap through the co-doping of Zr and Te highlight a successful method of tuning the electronic structure and band gap of $MgTiO_3$. This control over the band structure is vital for the charge carrier dynamics and light absorption processes, making it a potential candidate for optoelectronic applications and optical sensors. Such results confirm that the chemical and structural changes brought about by co-doping can considerably modify the electronic structure and optical properties of the material and provide excellent potential for advanced technological applications.

The TDOS and PDOS depicted in Figure 4 provide further insight into the evolution of electronic structure. The computed TDOS and PDOS for Zr- and Te-co-doped $MgTiO_3$ show the contribution of the atomic orbitals of the different elements to the electronic states and the energy level of the electronic transitions that occur from the VB to the CB of the material. The following results show that co-doping affects the electronic structure. Figures 4 show the and TDOS, respectively, of the pure and Zr/Te co-doped $MgTiO_3$. The TDOS is shown from -6 eV to 6 eV. In the case of $MgTiO_3$ being undoped, the VB mainly consists of O-p, while the CB consists of Ti-d. O-p and Ti-d orbitals hybridize to a high level toward suggesting that oxygen and titanium couple electronically in a strong way. Zr and Te co-doping additionally contributes to electronic coupling through extra orbitals and hybridizations, which causes changes to the electronic structure important for tuning functional properties.

Co-doping with Te and Zr considerably changes the electronic structure of $MgTiO_3$. The bottom of the valence band of (Te, Zr) co-doped $MgTiO_3$ lies in the range −5.5 to −4.5 eV and is dominated by the Te-p contribution. However, the VBM of (Te, Zr) co-doped $MgTiO_3$ is dominated by the O-p contribution with minor contributions from Mg, Ti, Zr, and Te s orbitals. A large hybridization of Te-p states with O-p states is displayed, which improves the mobility of carrier electrons and improves optical absorption. The CB is dominated by Ti-d orbitals, showing that the role of Ti in the electronic transitions in $MgTiO_3$ is important. The co-doping shifts the Fermi level towards the VBM and induces p-type SC characteristics due to the charge compensation effects of Zr and Te substitution. The Te-p states are situated at the VBM, and the Zr-d states are near the CBM, and this makes the band gap smaller as the VBM is elevated and the CBM is pushed down. The band gap narrowing was confirmed by the TDOS and PDOS, which shows that the defects generated by the presence of dopants narrowed the energy band gap between the VB and CB edges. These changes in the electronic structure indicate the suitability of (Te, Zr)-co-doped $MgTiO_3$ for optoelectronic applications.

Table 1. Calculated Eg of pristine and Zr/Te co-doped $MgTiO_3$ obtained using the TB-mBJ functional.

Materials	**Eg (eV)**
$\mathbf{MgTiO_3}$	2.93
$\mathbf{Mg_8Ti_7Zr_1O_{23}Te_1}$	1.15
$\mathbf{Mg_8Ti_7Zr_1O_{22}Te_2}$	0.64

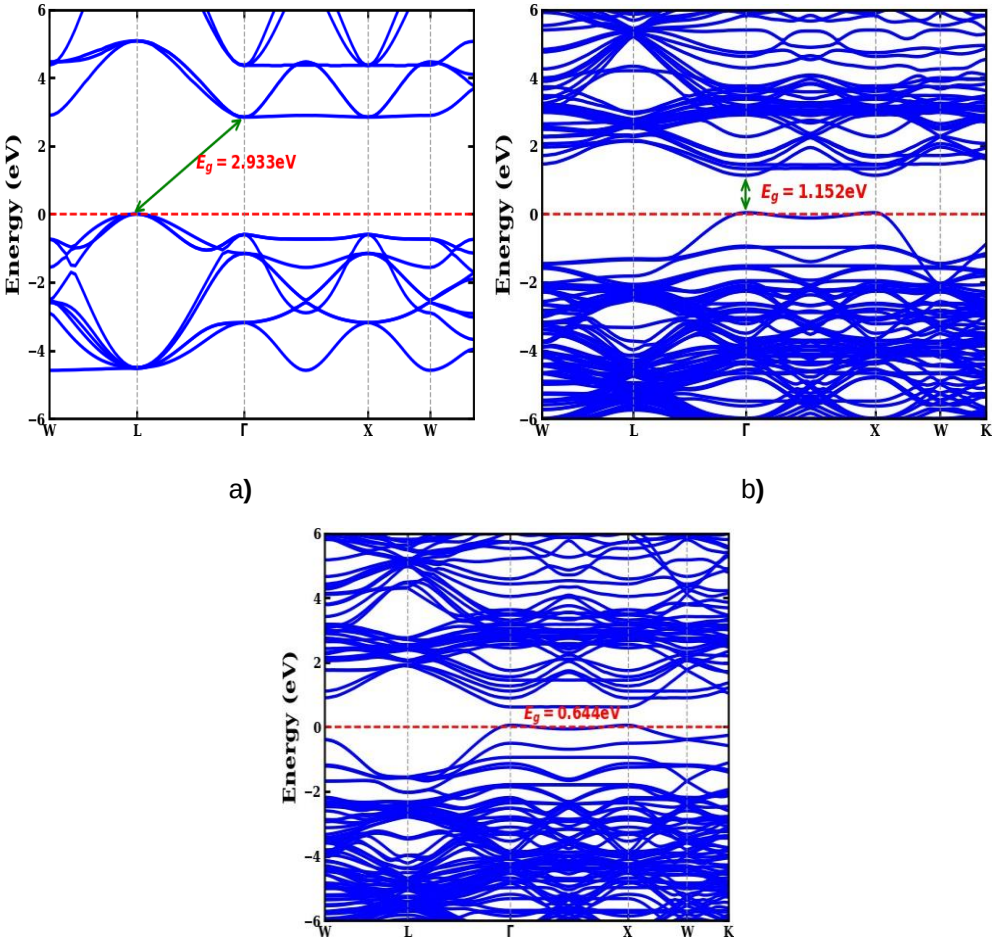

Figure 3: Electronic band structures of (a) pristine $MgTiO_3$, (b) (Zr, Te) co-doped $MgTiO_3$ with one Te atom, and (c) (Zr, Te) co-doped $MgTiO_3$ with two Te elements.

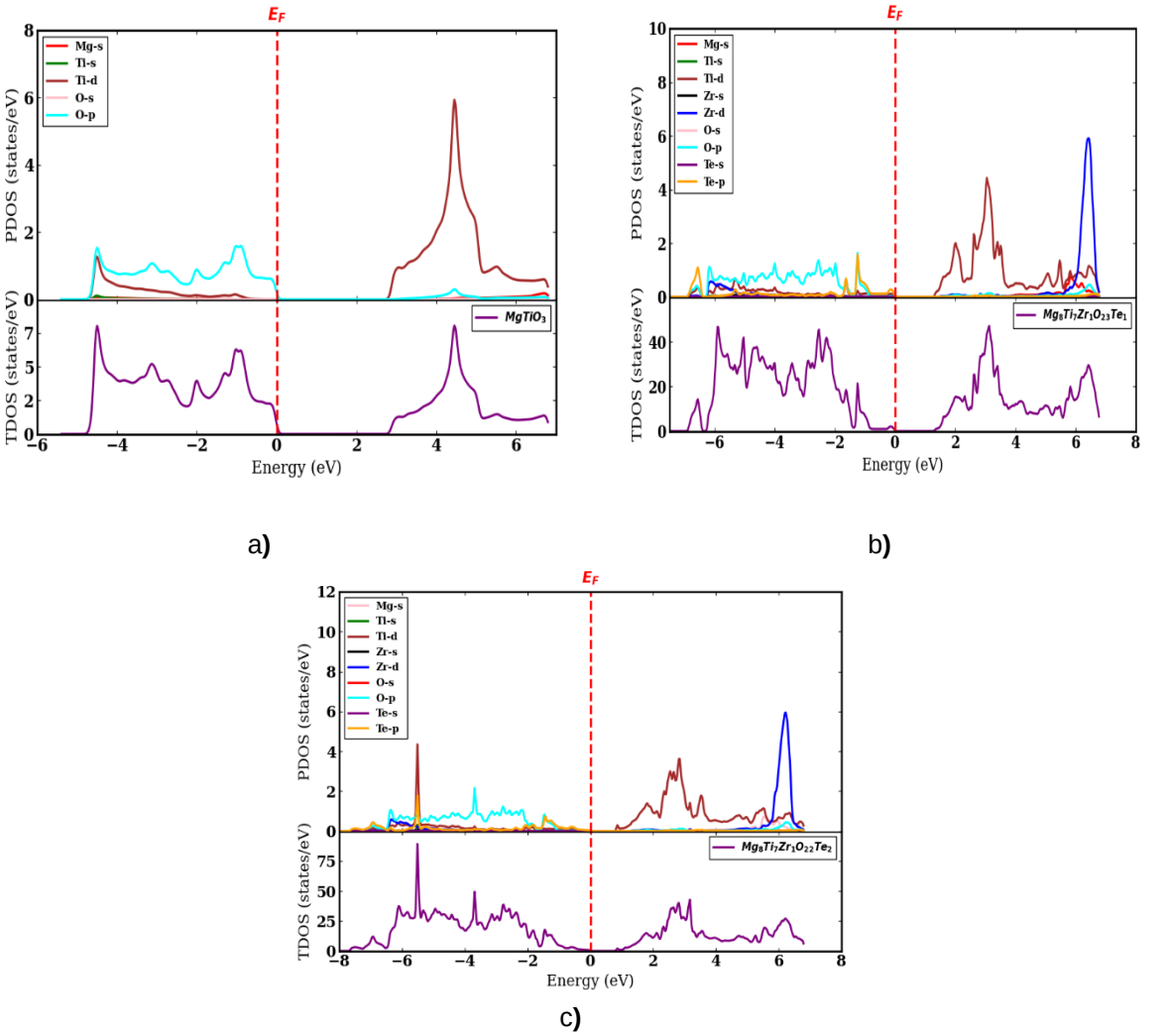

Figure 4: TDOS and PDOS of (a) pristine $MgTiO_3$, (b) (Zr, Te) co-doped $MgTiO_3$ with one Te atom, and (c) (Zr, Te) co-doped $MgTiO_3$ with two Te elements.

3.3. Optical properties:

The optical properties of pristine and (Zr, Te) co-doped $MgTiO_3$ were systematically investigated by analyzing the frequency-dependent complex DF $\varepsilon(\omega) = \varepsilon_1(\omega) + i\varepsilon_2(\omega)$, the optical absorption coefficient $\alpha(\omega)$, and the optical conductivity $\sigma(\omega)$. These quantities are crucial for understanding the interaction of electromagnetic radiation with matter and for assessing the potential of materials in optoelectronic applications.

The $\varepsilon_1(\omega)$ of the DF is presented in Figure 5(a). $\varepsilon_1(\omega)$ has a moderate value of the static dielectric constant $\varepsilon_1(0)$ in the case of pristine $MgTiO_3$ materials, which is a typical feature of wide band gap semiconductor oxides. When the materials are co-doped with (Zr, Te), a remarkable increase in the value of $\varepsilon_1(0)$ is found, especially in the direction

along the crystal axis zz. The $\varepsilon_2(\omega)$ of the DF for the given compound is presented in Figure 5(b) and represents the inter-band optical transitions. It should be noted that for the pristine compound of $MgTiO_3$, the onset of absorption is located in the ultraviolet region with an energy higher than 3.5 eV, as expected for such compounds with large band gaps. On the contrary, for the co-doped compounds with Zr and Te, the red shift of the onset of absorption to the range of visible light with an energy between 1.5 and 2.0 eV is observed due to optical transitions involving Te-p states near the VB and the Zr-d/Ti-d states near the CB. The $\alpha(\omega)$, as indicated in Figure 5(c), again verifies the aforementioned phenomenon. While pristine $MgTiO_3$ absorbs UV light and is nearly transparent in the visible spectrum, co-doping increases visible light absorption.

Figure 5(d) presents the $\sigma(\omega)$. For pristine $MgTiO_3$, $\sigma(\omega)$ remains nearly zero below 3 eV, indicating weak photon-induced charge transport. In contrast, the co-doped systems exhibit finite $\sigma(\omega)$ at lower photon energies, reflecting enhanced photogenerated charge carrier activity. The appearance of prominent conductivity peaks at reduced energies suggests that dopant-induced electronic states facilitate more efficient optical transitions.
Overall, the (Zr, Te) co-doping strategy significantly modifies the optical response of $MgTiO_3$, transforming it from a UV-active wide-bandgap into a visible-light-sensitive. The enhanced dielectric response, extended absorption range, and increased $\sigma(\omega)$ highlight (Zr, Te)-co-doped $MgTiO_3$ as a promising candidate for advanced technological applications.

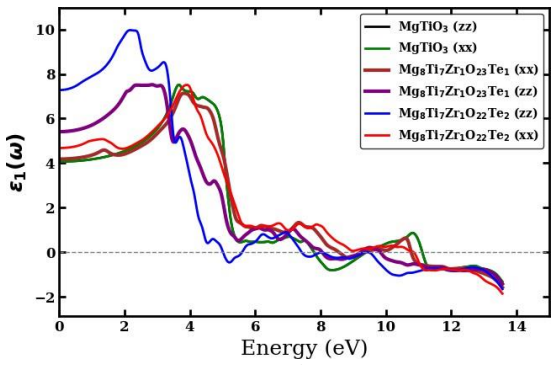

a)

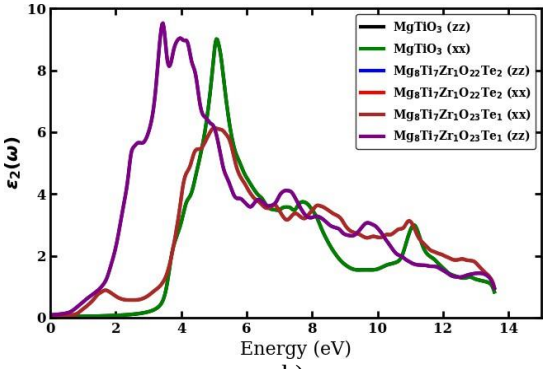

b)

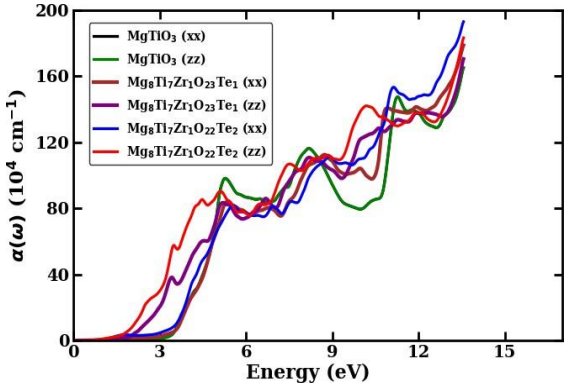

c)

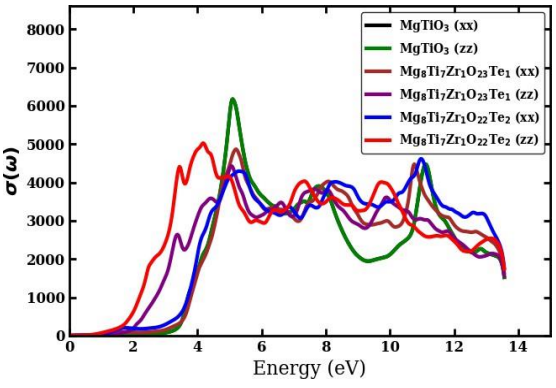

d)

Figure 5: Optical properties of pristine and (Zr, Te) co-doped $MgTiO_3$: (a) real and (b) imaginary parts of the DF, (c) optical absorption coefficient, and (d) optical conductivity as a function of photon energy.

4. Conclusion:

A first-principles study using DFT investigated the optoelectronic properties of pristine and (Zr, Te) co-doped $MgTiO_3$. Electronic structure analysis reveals that pure $MgTiO_3$ is a wide band gap material with limited visible light utilization. However, Zr/Te co-doping introduces impurity states near the VBM and CBM, narrowing the band gap and shifting optical activity from the ultraviolet to the visible range. Improved static dielectric constant, absorption edge, visible light absorption, and low-photon-energy optical conductivity in the co-doped material support these findings. These improvements arise from the hybridization of Te-p and Zr-d states with the host lattice, facilitating interband transitions and charge carrier excitation. In addition, (Zr, Te) co-doping effectively tunes the electronic and optical properties of $MgTiO_3$, enhancing its optical response and electronic transport, making it a promising candidate for advanced technological and optoelectronic applications. This theoretical work provides valuable guidance for experimental synthesis and devices. Although the present study is based on first-principles calculations, the predicted trends can be experimentally validated using well-established characterization techniques. Structural properties may be examined using X-ray diffraction (XRD), while the band gap and optical absorption can be measured using UV–Vis spectroscopy. In addition, photoluminescence spectroscopy can provide insights into recombination mechanisms and electronic transitions. Importantly, previous experimental studies on doped titanate perovskites have reported band gap narrowing and enhanced visible-light absorption upon doping, which are consistent with our theoretical predictions. Therefore, the present results provide reliable guidance for future experimental synthesis and characterization of Zr/Te co-doped $MgTiO_3$ for optoelectronic and energy-related applications.

Funding: The authors are warmly grateful to the support of “The Moroccan Association of Sciences and Techniques for Sustainable Development (MASTSD), Beni Mellal, Morocco”

References

[1] S. Nazir, I. Mahmood, N.A. Noor, A. Laref, M. Sajjad, Ab-initio simulations of MgTiO3 oxide at different pressure. High Energy Density Phys. 33, 100715 (2019). https://doi.org/10.1016/j.hedp.2019.100715

[2] F. Opoku, K.K. Govender, C.G.C.E. van Sittert, P.P. Govender, Recent progress in the development of semiconductor-based photocatalyst materials for applications in photocatalytic water splitting and degradation of pollutants. Adv. Sustain. Syst. 1, 1700006 (2017). https://doi.org/10.1002/adsu.201700006

[3] A. Cesana, E. Mauro, M. Silari, Induced radioactivity in a patient-specific collimator used in proton therapy. Nucl. Instrum. Methods Phys. Res. B 268, 2272–2280 (2010). https://doi.org/10.1016/j.nimb.2010.03.004

[4] S.E. Hosseini, M.A. Wahid, Hydrogen production from renewable and sustainable energy resources: Promising green energy carrier for clean development. Renew. Sustain. Energy Rev. 57, 850–866 (2016). https://doi.org/10.1016/j.rser.2015.12.112

[5] L. Azzouz, M. Halit, M. Rérat, R. Khenata, A.K. Singh, M.M. Obeid, X. Wang, Structural, electronic and optical properties of ABTe2 (A = Li, Na, K, Rb, Cs and B = Sc, Y, La): Insights from first-principles computations. J. Solid State Chem. 279, 120954 (2019). https://doi.org/10.1016/j.jssc.2019.120954

[6] A. Bouzaid, Y. Ziat, H. Belkhanchi, Photocatalytic optimization of $ATiO_3$ codoped with Se/Zr: A DFT study for hydrogen production. Materials 18, 4389 (2025). https://doi.org/10.3390/ma18184389

[7] Y. Ding, W. Que, J. He, W. Bai, P. Zheng, P. Li, J. Zhai, Realizing high-performance capacitive energy storage in lead-free relaxor ferroelectrics via synergistic effect design. J. Eur. Ceram. Soc. 42, 129–139 (2022). https://doi.org/10.1016/j.jeurceramsoc.2021.09.051

[8] Z. Li, L. Liu, B. Xu et al., High-contrast gratings based spoof surface plasmons. Sci. Rep. 6, 21199 (2016). https://doi.org/10.1038/srep21199

[9] T. Santhosh Kumar, P. Gogoi, A. Perumal, P. Sharma, D. Pamu, Effect of cobalt doping on the structural, microstructure and microwave dielectric properties of MgTiO3 ceramics prepared by semi-alkoxide precursor method. J. Am. Ceram. Soc. 97, 1054–1059 (2014). https://doi.org/10.1111/jace.12851

[10] A. Bouzaid, Y. Ziat, H. Belkhanchi, Ab initio design of Zr/Te co-doped $XTiO_3$ (X = Ca, Sr) perovskites for enhanced solar-driven hydrogen evolution and optoelectronic energy conversion. Next Mater. 11, 101666 (2026). https://doi.org/10.1016/j.nxmate.2026.101666

[11] K. Momma, F. Izumi, VESTA3 for three-dimensional visualization of crystal, volumetric and morphology data. J. Appl. Crystallogr. 44, 1272–1276 (2011). https://doi.org/10.1107/S0021889811038970

[12] F.D. Murnaghan, The compressibility of media under extreme pressures. Proc. Natl. Acad. Sci. USA 30, 244–247 (1944). https://doi.org/10.1073/pnas.30.9.244

[13] A.A. Adewale, A. Chik, T. Adam, O.K. Yusuff, S.A. Ayinde, Y.K. Sanusi, First principles calculations of structural, electronic, mechanical and thermoelectric properties of cubic ATiO3 (A = Be, Mg, Ca, Sr and Ba) perovskite oxide. Comput. Condens. Matter 28, e00562 (2021). https://doi.org/10.1016/j.cocom.2021.e00562